Molecular Crystals and Liquid Crystals

ISSN: 1542-1406 (Print) 1563-5287 (Online) Journal homepage: http://www.tandfonline.com/loi/gmcl20

Liquid-Crystalline and Electronic Properties of Racemic-Alkoxy Chains-Substituted Tetraazanaphthacene

Tomonori Abe, Mitsuru Matsuzaka, Kyosuke Isoda & Makoto Tadokoro

To cite this article: Tomonori Abe, Mitsuru Matsuzaka, Kyosuke Isoda & Makoto Tadokoro (2015) Liquid-Crystalline and Electronic Properties of Racemic-Alkoxy Chains-Substituted Tetraazanaphthacene, Molecular Crystals and Liquid Crystals, 615:1, 70-77, DOI: 10.1080/15421406.2015.1066963

To link to this article: http://dx.doi.org/10.1080/15421406.2015.1066963

Mol. Cryst. Liq. Cryst., Vol. 615: pp. 70–77, 2015

ISSN: 1542-1406 print/1563-5287 online
DOI: 10.1080/15421406.2015.1066963

Liquid-Crystalline and Electronic Properties of Racemic-Alkoxy Chains-Substituted Tetraazanaphthacene

TOMONORI ABE, MITSURU MATSUZAKA, KYOSUKE ISODA,* AND MAKOTO TADOKORO*

Department of Chemistry, Faculty of Science, Tokyo University of Science, Shinjuku-ku, Tokyo, Japan

*We have prepared tetraazanaphthacene-based liquid crystal **1** having two racemic alkoxy chains. Compound **1** self-organizes to form the rectangular columnar liquid-crystalline phase over a wide temperature range including room temperature. However, compound **2** having two linear alkoxy chains is incapable of self-organizing superstructures. Since cyclic voltammetry revealed that **1** has two-step and two-electron reductions, **1** is expected to function as electron-transporting material.*

Keywords *N*-heteroacene; electron acceptor; redox-active; rectangular columnar LC phase

Introduction

Molecular assembly formed by self-organization of design-programmed molecules for non-covalent intermolecular interactions such as a hydrogen and a coordination bonding, an electrostatic interactions, and a van der Waals force can fabricate into the formation of the highly ordered superstructures in the bulk materials.[1–5] Liquid-crystalline (LC) molecules can form self-organized nanostructures in thin films unlike amorphous materials because an arrangement of molecules in LC states already adapts an ordered superstructure by intermolecular interactions such as a hydrophobic interaction of long alkyl chains.[6–8] Design-Programmed LC molecules composed of π-conjugated frameworks and long alkyl chains can self-organize into 1- and 2-dimensional ordered nanostructures, which are expected to transport charge carriers such as electron and hole via the overlap of π-orbitals between neighbouring π-conjugated moieties.[13,14] Moreover, a self-healing behaviour of LC materials reduces grain boundary and structural defects by molecular fluctuation, which is an efficient advantage compared to the crystalline materials.[19,20] For these reasons, LC molecules based on hole-transporting oligothiophene,[10,11] triphenylene,[9] and hexabenzocoronene derivatives[15,16] have been prepared and applied into the field-effect transistors (FETs), light-emitting diode (LEDs), and photovoltaic

*Address correspondence to Kyosuke Isoda, and Makoto Tadokoro, Department of Chemistry, Faculty of Science, Tokyo University of Science, 1-3 Kagurazaka, Shinjuku-ku, Tokyo 162-8601, Japan. E-mail: k-isoda@rs.tus.ac.jp; tadokoro@rs.kagu.tus.ac.jp

Color versions of one or more of the figures in the article can be found online at www.tandfonline.com/gmcl.

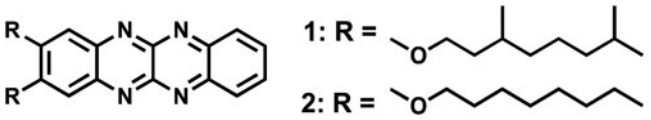

Figure 1. Molecular structures of **1** and **2**.

cells. On the other hand, the developments of electron-transporting LC molecules are still limited except for hexaazatriphenylene,[17] perylene tetracarboxylic bisimide,[18] and fullerene derivatives.[19] We have recently focused on π-conjugated *N*-heteroacene derivatives as the building block for the development of the novel electron-transporting LC molecules.

N-heteroacene, in which N atoms partially substitute C atoms in a π-conjugated polycyclic oligoacene, behaves as an electron accepter owing to the presence of electron deficient imino-*N* atoms.[20,21] We have previously reported on an electron-accepting 5,6,11,12-tetraazanaphthacene (TANC) as *N*-heteroacene, which have reversible two-step and two-electron reduction peaks ($E^1_{1/2}$ = –0.66 V and $E^2_{1/2}$ = −1.20 V *vs.* Ag/Ag$^+$).[22–24] TANC-based thin films prepared by a vapour deposition show the electron mobility of 8.9×10^{-5} cm^2 V^{-1}s^{-1} by the FET measurements,[22] whereas the FET activity decreases because of the growth of the independent and isolated crystalline domains on the surface overtime. For the improvement of electro-active character in the crystalline films of TANC molecules, we have introduced the LC property into π-conjugated TANC framework to show more efficient electron-transporting properties. Until now, we have prepared the LC TANC derivative showing the hexagonal columnar (Col_h) LC phase over a wide temperature range including room temperature.[25] For the fabrication of the LC materials working as the essential electron-transporting properties, it is important work to synthesize a series of modified LC TANC derivatives.

Herein, we report on the LC TANC derivative self-organizing to form the columnar LC structure, which is different from the Col_h LC phase. Molecular structures of compound 1 and 2 having two racemic or linear alkoxy chains on the π-conjugated TANC frameworks, respectively, are shown in Fig. 1. In this study, we found that self-organized LC structures can be controlled by tuning the length of racemic alkoxy chains substituted into TANC framework. The introduction of two shorter racemic alkoxy chains into the TANC framework leads to the formation of the rectangular columnar (Col_r) LC phase for 1 in a wide temperature range including room temperature. To the best of our knowledge, this is the first time on the Col_r LC TANC derivative.

Results and Discussion

Compounds 1 and 2 have been prepared according to our previous procedure.[25] The thermal behaviour of 1 and 2 are summarized in Table 1. Polarized optical microscopic observation of 1 has shown a fan-like texture with a large extinction along the polarizer directions, characteristic of the columnar (Col) LC phase at room temperature in Fig. 2. Differential scanning calorimetry (DSC) has revealed that 1 shows the Col LC phase in a wide temperature range including room temperature in Fig. 3. The phase transition peak of 1 from the Col LC phase to isotropic liquid on heating is clearly observed at 98.0°C. On the other hand, the phase transition temperature of 2 from crystalline phase to isotropic liquid is 181.0°C, which is much higher than that of LC TANC derivative 1. Compared

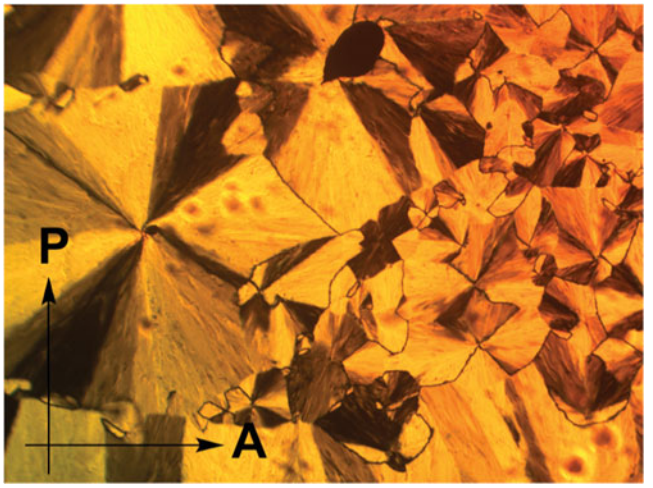

Figure 2. Polarized optical micrograph of **1** in the Col_r LC phase at room temperature on cooling. Arrows indicate the directions of polarizer (P) and analysis (A) axes.

to linear alkoxy chains for 2, the substitution of highly fluid branched-alkoxy chains for 1 lowers a melting point as well as makes TANC molecules more flexible. As a result, the nanosegregation between flexible branched-alkoxy chains and rigid TANC frameworks should play a role to stabilize the formation of the Col LC structure for 1.[12,25,26]

The X-ray diffraction (XRD) pattern of compound 1 measured at room temperature is shown in Fig. 4a. The XRD pattern of 1 shows four reflection peaks at 26.9, 21.3, 17.3, 14.6, 13.5, 12.5, 8.98, 7.20, 7.08, and 6.72 Å in the small-angle region, which can be assigned as Miller indices (110), (200), (020), (300), (220), (310), (420), (600), (050), and (440), respectively. This result should indicate that compound 1 self-organize to form the Col_r LC phase with $P2_1/a$ symmetry,[27] of which rectangular lattice constants are $a = 53.8$ Å and $b = 23.2$ Å (Figure 4a). In the column, each neighbouring TANC frameworks of 1 would be arranged in a head-to-head manner with H-bonds of a CH···N type to form a 1D π-stacking column, similar to the Col_h LC phase for LC TANC derivative with longer racemic alkoxy chains (Figure 4b).[25] It should be noted that the decrease in a length of branched-alkoxy chains attached on TANC framework should lower the molecular mobilities for 1, resulting in the generation of stronger interaction between TANC cores in the column of 1. The disc-like assembly formed by compound 1 adopted an elliptical shape along the column axis, and the this assembly should be tilted within the columns. The tilted column in the

Table 1. Phase transition behavior of **1** and **2**

Compound	Phase transition [a]
1	[b] Col_r 98.0 (13.0) Iso
2	[b] Cr 181.0 (6.9) Iso

[a] Phase transition temperatures (°C) and enthalpy changes in parentheses ($kJ \cdot mol^{-1}$) determined by DSC on a second cycle at the scanning velocity of 10 °C min^{-1}. Col_r: rectangular columnar; Cr: crystalline; Iso: isotropic. [b] No distinct transition peaks are detected on DSC measurement below –50 °C.

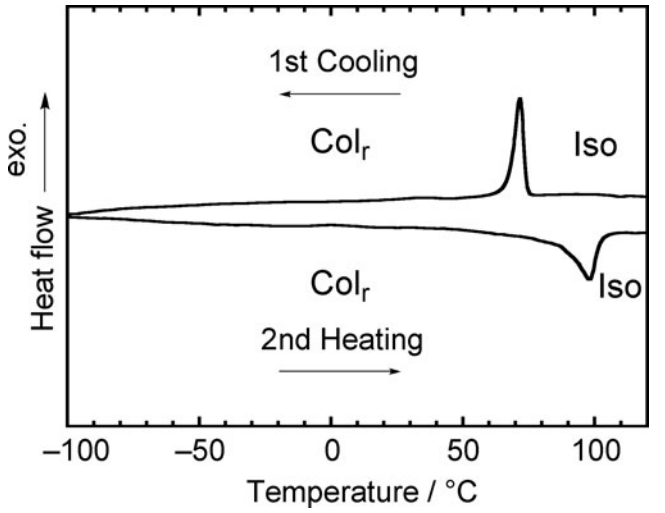

Figure 3. DSC thermogram of **1** at a scanning rate of 10 °C min^{-1}. Col$_r$: rectangular columnar; Iso: isotropic.

Col$_r$ phase for 1 allowed closer contacts between the cores formed by TANC frameworks. Moreover, the fully extended molecular length of 1 in the column is estimated to be *ca.* 46 Å, which is longer than *b* value. This result indicates that the interdigitation of alkyl chains between the neighbouring columns of 1 also should occur in the Col$_r$ LC phase.

The electronic properties of compound 1 have evaluated by UV–*vis* and cyclic voltammetry (CV) measurements. The UV–*vis* spectrum of compound 1 shows the lowest energy absorption maximum at 440 nm in CH_2Cl_2 in Fig. 5a. Cyclic voltammogram of 1 in CH_2Cl_2 solution with 0.10 M nBu$_4$NPF$_6$ shows reversible two-step and two-electron reductions in Figure 5b. These two redox potentials of 1 are observed at $E_{1/2}$ = –0.87 V and –1.21 V (*vs.* Ag/Ag$^+$), of which these reductions are assigned to the formation of the radical anion and the dianion of the TANC framework, respectively.[23] The LUMO and HOMO energy levels (E_{LUMO} and E_{HOMO}) of 1 can be approximately estimated from

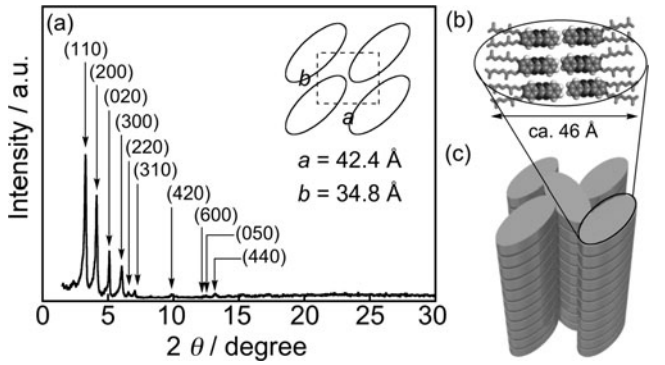

Figure 4. (a) X-Ray diffraction pattern and schematic illustration of **1** in the disc-like assembly (b) in the Col$_r$ LC phase (c) at room temperature.

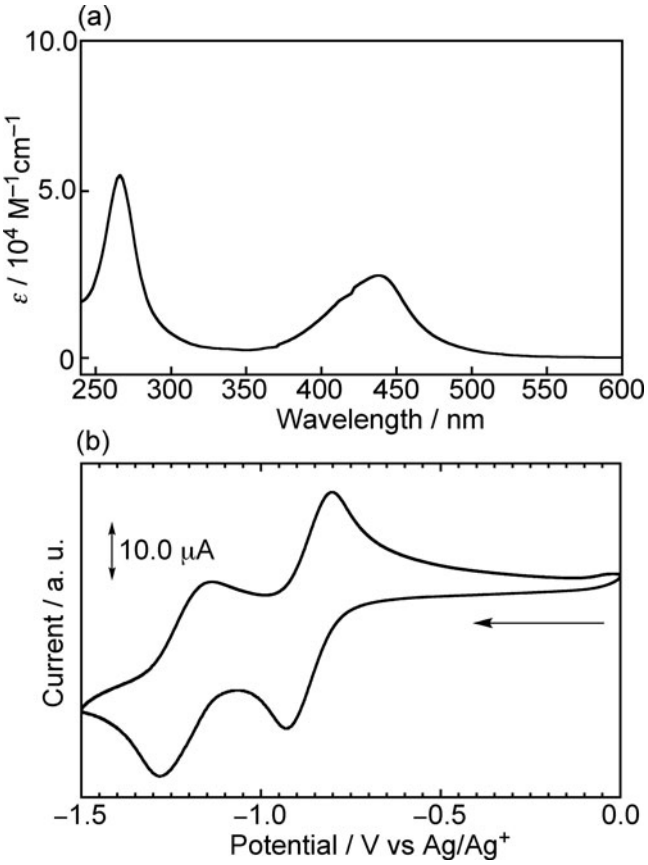

Figure 5. (a) UV–*vis* spectrum of **1** in CH_2Cl_2 and (b) cyclic voltammogram of **1** at 1.0 mM in CH_2Cl_2 solution of nBu$_4$NPF$_6$ (0.10 M) at a scanning velocity of 100 m Vs^{-1}.

Table 2. Spectroscopic and electrochemical data of **1**

	UV–*vis* λ_{max} [nm]	Redox potential[a] $E^1_{1/2}$	$E^2_{1/2}$	E_{LUMO}[b] [eV]	E_{HOMO}[c] [eV]	E_g^{opt} [d] [eV]
1	267, 440	–0.87	–1.21	–3.71	–6.29	2.58

[a] Measured by cyclic voltammetry in CH_2Cl_2 solution of nBu$_4$NPF$_6$ (0.10 M). The redox potential of ferrocene as an internal reference is observed at $E^1_{1/2} = 0.20$ V. [b] E_{LUMO} is calculated from first half-wave potential ($E^1_{1/2}$) with the assumption that the energy level of ferrocene is −4.8 eV below vacuum level: $E_{LUMO} = -E^1_{1/2} - 4.8$ eV. [c] E_{HOMO} is calculated by the equation: $E_{HOMO} = E_{LUMO} - E_g^{opt}$. [d] Estimated from the onset position of the UV–v*is* absorption spectrum in CH_2Cl_2: $E_g^{opt} = 1240 / \lambda_{onset}$.

the $E_{1/2}$ potential in the cyclic voltammogram and the absorption edge of UV–*vis* spectrum, respectively in Table 2. The E_{LUMO} of alkoxy-substituted TANC for 1 is as same as –3.71 eV, which is higher than that of unsubstituted TANC molecule ($E_{LUMO} =$ –4.00 eV). These results should be due to the substitution of two electron-donating alkoxy moieties into electron-accepting TANC framework. Since the E_{LUMO} of 1 is almost similar to those of LC fullerene,[19] LC hexaazatriphenylenes,[17] and LC perylene tetracarboxylic acid bisimide derivatives,[18] compound 1 is expected to function as *n*-type LC semiconductors based on their electron-accepting properties. The electron-transporting properties of a series of LC TANC derivatives are currently underway.

Conclusion

In conclusion, we have synthesized LC TANC derivative 1 as *N*-heteroacene. Compound 1 comprises in two racemic alkoxy-chains and a π-conjugated framework, which shows the Col_r LC phase in a wide temperature range including a room temperature. Cyclic voltammetry revealed that redox-active 1 behaves as the electron-accepting properties due to the occurrence of the two-step and two-electron reductions. Since LC TANC derivative 1 provides us new information to tune self-organized superstructures formed by the TANC derivative, we prepare a series of LC TANC derivatives which can transport carrier as electron in progress.

Samples

2,3-(3,7-dimethyl-1-octyloxy)-5,6,11,12-tetraazapentacene (1)

^{1}H NMR (300 MHz, $CDCl_3$):δ 8.93(m, 2H), 7.91(m, 2H), 7.40(m, 2H), 4.34(m, 4H), 1.80–0.98(m, 20H), 0.91–0.84(m, 18H) ppm; ^{13}C NMR (75 MHz, $CDCl_3$): δ 157.08, 147.61, 145.63, 143.27, 131.42, 129.95, 104.87, 68.28, 39.18, 37.27, 35.45, 30.04, 27.95, 24.71, 22.69, 22.59, 19.67 ppm; IR(ATR): $\nu =$ 2951, 2924, 2844, 1728, 1616, 1552, 1485, 1446, 1385, 1346, 1311, 1232, 1182, 1122, 1078, 1043, 968, 879, 842, 757, 719, 555, 515 cm^{-1}; MS(FAB-MS): m/z calcd: 544.77 $[M+H]^+$; found: 545.29; elemental analysis: calcd (%) for CHNO: C 74.96, H 8.88, N 10.28; found: C 74.92, H 9.01, N 9.93.

2,3-(dioctyloxy)- 5,6,11,12-tetraazapentacene (2)

^{1}H NMR (300 MHz, $CDCl_3$):δ 8.38(dd, $J =$ 3.3, 6.6 Hz, 2H), 7.91(dd, $J =$ 3.3, 6.6 Hz, 2H), 7.38 (s, 2H) 4.30(t, $J =$ 6.3 Hz, 4H), 2.02(quint, $J =$ 6.3 Hz, 4H), 1.80–0.98(m, 20H), 0.89(t, $J =$ 6.3 Hz, 6H) ppm; ^{13}C NMR (75 MHz, $CDCl_3$): δ 157.13, 147.62, 145.64, 143.28, 131.43, 129.96, 104.90, 68.80, 31.78, 29.28, 29.25, 27.98, 28.59, 25.99, 22.62, 14.10 ppm; IR(ATR): $\nu =$ 2952, 2916, 2850, 1722, 1624, 1556, 1485, 1458, 1387, 1342, 1230, 1176, 1119, 1052, 1011, 993, 897, 852, 829, 758, 719, 557, 515 cm^{-1}; MS(MALDI-TOF-MS): m/z calcd: 488.66 $[M+H]^+$; found: 489.37; elemental analysis: calcd (%) for CHNO: C 73.74, H 8.25, N 11.47; found: C 73.14, H 8.11, N 11.28.

General Method

^{1}H and ^{13}C NMR spectra were recorded on a JEOL JNM-LA300 spectrometer. Chemical shift of ^{1}H and ^{13}C NMR signals were quoted to tetramethylsilane ($\delta = 0.00$) and ($\delta = 77.00$)

as internal standards, respectively. IR spectra were measured with a HORIBA FREEXACT-II spectrometer. MALDI-TOF mass spectra were collected on a JEOL JMS-S3000 by using dithranol as matrix. Elemental analyses were carried out with Perkin-Elmer instruments Series II CHNS/O Analyzer 2400. Cyclic voltammetry (CV) was carried out in CH_2Cl_2 solution of Bu_4NPF_4 (0.10 M) with glassy carbon working, Pt counter, and an Ag/Ag^+ reference electrode using an ALS CHI 600B electrochemical analyzer. All potential were calibrated with Fc/Fc^+ couple using ferrocene as an internal reference. UV–*vis* absorption spectra were measured with a JASCO V-550 UV–*vis* Spectrophotometer spectrometer. DSC measurements were performed on a Bruker DSC3200SA at a scanning rate of 10 °C min^{-1}. The phase transition temperatures were taken at the top of transition peaks in the DSC traces. XRD patterns were obtained using a Rigaku RINT-2500 diffractometer with a heating stage using Ni-filtered Cukα radiation. A Nikon OPTIPHOTO-POL polarizing optical microscope equipped with a Mettler FP90/82HT hot stage was used for visual observation of optical textures. All reagents and solvents were purchased from Aldrich, Tokyo Kasei, Kanto Chemical, or Wako, and used as received.

Funding

This work was supported by a Grant-in-Aid for Scientific Research on Innovative Areas of "New Polymeric Materials Based on Element-Blocks (No. 2401)" (no. 25102540, K.I.) from the Ministry of Education, Culture, Sports, Science, and Technology of Japan; The Ogasawara Foundation for the Promotion of Science & Engineering (K.I.); and The Hattori Hokokai Foundation (K.I.); Nippon Sheet Glass Foundation for Materials Science and Engineering (K.I.); Futaba Electronics Memorial Foundation (K.I.).

References

[1] Hoeben, F. J. M., Jonkheijm, P., Meijer, E. W., & Schenning, A. P. H. J. (2005). *Chem. Rev.*, *105*, 1491.
[2] Storhoff, J. J., Mirkin, C. A. (1999). *Chem. Rev.*, *99*, 1849.
[3] Northrop, B. H., Zheng, Y. R., Chi, K. W., Stang, P. J. (2009). *Acc. Chem. Res.*, *42*, 1554.
[4] Hartgerink, J. D., Beniash, E., Stupp, S. I. (2001). *Science*, *294*, 1684.
[5] Pisula, W., Feng, X., Müllen, K. (2010). *Adv. Mater.*, *22*, 3634.
[6] Demus, D., *et al.* (1998). *Handbook of Liquid Crystals*, Wiley-VCH: Weinheim.
[7] Kato, T., Mizoshita, N., Kishimoto, K. (2006). *Angew. Chem. Int. Ed.*, *45*, 38.
[8] Sergeyev, S., Pisula, W., Geerts, Y. H. (2007). *Chem. Soc. Rev.*, *36*, 1902.
[9] Adam, D., Schuhmacher, P., Simmerer, J., Häussling, L., Siemensmeyer, K., Etzbach, K. H., Ringsdorf, H., Haarer, D. (1994). *Nature*, *371*, 141.
[10] Funahashi, M., Hanna, J. (2005). *Adv. Mater.*, *17*, 594.
[11] Yasuda, T., Ooi, H., Morita, J., Akama, Y., Minoura, K., Funahashi, M., Shimomura, T., Kato, T. (2009). *Adv. Funct. Mater.*, *19*, 411.
[12] Isoda, K., Yasuda, T., Kato, T. (2009). *Chem. Asian. J.*, *9*, 1619.
[13] Cornil, J., Lemaur, V., Calbert, J. P., Brédas, J. L. (2002). *Adv. Mater.*, *14*, 726.
[14] Benito-Hernández, A., Pandey, U. K., Cavero, E., Termine, R., García-Frutos, E. M., Serrano, J. L., Golemme, A., Gömez-Lor, B. (2013). *Chem. Mater.*, *25*, 117.
[15] Xiao, S., Myers, M., Miao, Q., Sanaur, S., Pang, K., Steigerwald, M. L., Nuckolls, C. (2005). *Adv. Mater.*, *44*, 7390.
[16] Kastler, M. M., Laquai, F., Müllen, K., Wegner, G., (2006). *Appl. Phys. Lett., 89*, 252103.
[17] Gao, B., Zhang, L., Bai, Q., Li, Y., Yang, J., Wang, L., (2012). *New J. Chem.*, *34*, 2735.
[18] Funahashi, M., Sonoda, A., (2012). *J. Mater. Chem.*, *22*, 25190.

[19] Nakanishi, T., Shen, Y., Wang, J., Yagai, S., Funahashi, M., Kato, T., Fernandes, P., Möhwald, H., Kurth, D. G., (2008). *J. Am. Chem. Soc.*, *130*, 9236.
[20] Bunz, U. H. F., Engelhart, J. U., Lindner, B. D., Schaffroth, M., (2013). *Angew. Chem. Int. Ed.*, *52*, 2.
[21] Miao, Q., (2012). *Synlett*, *23*, 326.
[22] Tadokoro, M., Yasuzuka, S., Nakamura, M., Shinoda, T., Tatenuma, T., Mitsumi, M., Ozawa, Y., Toriumi, K., Yoshino, H., Shiomi, D., Sato, K., Takui, T., Mori, T., Murata, K., (2006). *Angew. Chem., Int. Ed.*, *45*, 5144.
[23] Isoda, K., Nakamura, M., Tatenuma, T., Ogata, H., Sugaya, T., Tadokoro, M., (2012). *Chem. Lett.*, *41*, 937.
[24] Tadokoro, M., Nakamura, M., Anai, T., Shinoda, T., Yamagata, A., Kawabe, Y., Sato, K., Shiomi, D., Takui, T., Isoda, K., (2011). *ChemPhysChem*, *12*, 2561.
[25] Isoda, K., Abe, T., Tadokoro, M., (2013). *Chem. Asian. J.*, *8*, 2951.
[26] Kato, T., (2002). *Science*, *295*, 2414.
[27] Laschat, S., Baro, A., Steinke, N., Giesselmann, F., Hägele, C., Scalia, G., Judele, R., Kapatsina, E., Sauer, S., Schreivogel, A., Tosoni, M., (2007). *Angew. Chem. Int. Ed.*, *46*, 4832.